

# Scalable quantum information processing with atomic ensembles and flying photons

Feng Mei,<sup>1</sup> Mang Feng,<sup>2,3\*</sup> Ya-Fei Yu,<sup>1,†</sup> and Zhi-Ming Zhang<sup>1,3‡</sup>

<sup>1</sup>*Laboratory of Photonic Information Technology, SIPSE & LQIT,  
South China Normal University, Guangzhou 510006, China*

<sup>2</sup>*State Key Laboratory of Magnetic Resonance and Atomic and Molecular Physics,  
Wuhan Institute of Physics and Mathematics, Chinese Academy of Sciences, Wuhan 430071, China*

<sup>3</sup>*Centre for Quantum Technologies and Department of Physics,  
National University of Singapore, 3 Science Drive 2, Singapore 117543, Singapore*

(Dated: October 26, 2018)

We present a scheme for scalable quantum information processing (QIP) with atomic ensembles and flying photons. Using the Rydberg blockade, we encode the qubits in the collective atomic states, which could be manipulated fast and easily due to the enhanced interaction, in comparison to the single-atom case. We demonstrate that our proposed gating could be applied to generation of two-dimensional cluster states for measurement-based quantum computation. Moreover, the atomic ensembles also function as quantum repeaters useful for long distance quantum state transfer. We show the possibility of our scheme to work in bad cavity or in weak coupling regime, which could much relax the experimental requirement. The efficient coherent operations on the ensemble qubits enable our scheme to be switchable between quantum computation and quantum communication using atomic ensembles.

PACS numbers: 03.67.Lx, 42.50.Pq

## I. INTRODUCTION

Recently, much effort has been paid on ensembles of trapped atoms as promising candidates for quantum state engineering and quantum information processing (QIP), such as realization of quantum repeater [1, 2, 3], storage and generation of photonic states [4, 5, 6, 7, 8, 9], and entanglement generation of the collective degrees of freedom in separate atomic ensembles [10, 11, 12]. Due to no need of addressing atoms individually and to the enhanced interaction with light, the atomic ensemble qubits seem superior to the single-particle qubits in QIP. However, the interface between the atomic ensemble and the light based on Raman scattering in above schemes requires the state of the atomic ensemble to be transformed into a photon travelling in a well-defined direction within a well-controlled period of time. More importantly, it is experimentally more challenging to achieve universal operations for QIP than quantum communication [13, 14, 15, 16] between different atomic ensemble qubits by interfacing collective atomic excitations with single photon pulses.

An attractive technique for a nontrivial two-qubit gating between atomic ensembles has been proposed in [17], in which the dipole-dipole interaction between highly excited Rydberg states blocks transitions of more than one Rydberg excitation. This is called the Rydberg blockade [18], which has been observed in clouds of cold atoms [19, 20, 21, 22, 23, 24, 25] as well as in a Bose-Einstein Condensate [26]. There have been a number of propos-

als to use the Rydberg blockade for various QIP tasks [27, 28, 29, 30, 31, 32, 33], most of which, however, are hard for scaling to a large numbers of qubits required for a working QIP. One of the main problems for scalability is that the Rydberg blockade only produces effective interaction within a certain interaction range. Although it is possible to interconnect two distant qubits by repeated using swap operations between neighboring qubits, the error threshold for swap operations would much suppress the scalability [34].

Together with the state-of-the-art techniques in cavity quantum electrodynamics [35, 36] and the recent impressive experimental advance for Rydberg blockade [37, 38], we put forward a scalable ensemble-based QIP scheme with the collective states of the atomic ensembles encoding the qubits and the flying photons as ancillas. Making use of the single-photon input-output process [39, 40], we employ optical cavities with each confining an atomic ensemble under the far-off-resonant interaction, which could produce a phase flip for each input single-photon pulse, and thereby could be extended to controlled quantum gating between different atomic ensemble qubits. We will show that the gating is insensitive to the Rydberg blockade error and also to the variation of the coupling rate  $g$  even if the atoms are not well localized within the Lamb-Dicke regime. Our scheme is also robust to the errors due to the photon loss from the atomic spontaneous emission, the photon collection and the detection inefficiency, because the photon loss only reduces the success rate of the gating but has no affect on the fidelity of the gating under our measurement. In addition, the building block of our scheme could be readily used to generate cluster states with two-dimensional (2D) lattice geometry and to carry out conditional gating between two remote qubits. Moreover, we will show the availability of our scheme in different conditions, e.g., in the good or bad

\*E-mail: mangfeng@wipm.ac.cn

†E-mail: yfyuks@hotmail.com

‡E-mail: zmzhang@snu.edu.cn

cavity and in weak or strong coupling regime.

Our scheme has following advantages. (i) The entanglement between two atomic ensemble qubits is achieved by a single photon flying sequentially through two cavities confining the two atomic ensemble qubits respectively. This process is intrinsically of higher success rate than those based on coincident detection of two emitting photons going through a polarizing beam splitter (PBS). (ii) Compared to the single atom cases, the enhancement of the coherent coupling by  $\sqrt{N}$  in our scheme, with  $N$  the number of the atoms in the ensemble, could somewhat relax the experimental requirement. This also enables fast qubit rotation and the efficient readout in our scheme, useful for measurement-based quantum computation. Our atomic ensembles in the cavities can also function as good quantum repeaters for long-distance quantum communication [1, 2, 3]. As a result, quantum computation and quantum communication are readily switchable with each other in our system. (iii) Compared with a previous proposal [31] for generation of atomic ensemble cluster state, our scheme is more efficient and the repetition attempts only scale up polynomially with the atomic ensemble qubit number. (iv) Our scheme can work well under wide range of experimental parameters, where the quantum gating associated with the case of the weak coupling or large cavity decay is made by means of the Faraday rotation.

The paper is structured as follows. The next section focuses on the interaction between a single-photon pulse and an atomic ensemble in an optical cavity, which yields a controlled phase flip (CPF) gating. The single-photon pulse going through different spatially separate cavities could lead to entanglement and quantum gating between the confined atomic ensembles, as discussed in Section III. We will consider in Sections IV and V the experimental feasibility of our scheme and the possibility of our scheme working in the weak coupling regime or in bad cavity. The last section is for a short summary.

## II. OUR IDEA AND OPERATIONS

### A. Rydberg blockade regime and logical qubit encoding

The Rydberg blockade [17, 18] relies on the interaction between the atoms in the ensemble, which is intrinsically of the weak  $R^{-5}$  or  $R^{-6}$  van der Waals type in the absence of external electric field with  $R$  the distance between the atoms. Under an external electric field, however, the interaction would be much enhanced because the Rydberg states own permanent dipole moments  $\mu \sim n^2 ea_0$ , with  $n$  the principal quantum number,  $e$  the electronic charge and  $a_0$  the Bohr radius. Unfortunately, if the two atoms  $i$  and  $j$  are fixed, it has been found [41] that the interaction would be vanishing when the angle  $\theta_{ij}$  between the interatomic separation  $\mathbf{R}$  and the electric field  $\mathbf{E}$  approaches  $\arccos(1/\sqrt{3})$ . In

the case of an atomic ensemble with  $N$  identical atoms within the blockade range, however, it is not practical to fully avoid  $\theta_{ij}$  ( $i, j \in [1, N], j > i$ ) =  $\arccos(1/\sqrt{3})$  for each atoms to get available Rydberg blockade. Nevertheless, we might employ Föster process, which could yield an isotropic Rydberg atom interaction of comparable strength  $R^{-3}$  [41] even in the absence of external electric field. In this process, if there exists a degeneracy in the energy level structure, i.e.  $nlj+nlj \rightarrow n'l'j'+n''l''j''$ , the interaction between the Rydberg atoms will be resonantly enhanced. Despite this, we should avoid choosing the Föster zero states by taking  $l' = l'' = l + 1$  and  $j' = j'' = j + 1$  [42].

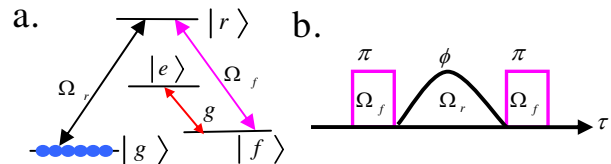


FIG. 1: (Color online) (a) The relevant level structure of the atoms in the ensemble. The atomic transition  $|g\rangle$  ( $|f\rangle$ )  $\rightarrow$   $|r\rangle$  is driven by the classical laser with the Rabi frequency  $\Omega_r(t)$  ( $\Omega_f(t)$ ), and  $|f\rangle \rightarrow |e\rangle$  is resonantly coupled to the cavity mode with a coupling rate  $g$ . (b) A sequence of laser pulses for a single logical qubit rotation.

In our scheme, the Rydberg blockade is utilized to generate the single excited symmetric atomic state and to rotate the single qubit state. The interaction for the blockade is at Föster resonance. Fig. 1(a) shows the relevant levels of each atom in the atomic ensemble with the metastable lower states  $|g\rangle$  ( $|f\rangle$ ) for long-time storage of qubit information and the high-lying Rydberg state  $|r\rangle$  and the excited state  $|e\rangle$  for ancillas. Assuming that all the atoms have been cooled to micro-Kelvin and prepared in the ground state  $|g\rangle$  in a far off-resonant optical trap (FORT). We define the logic qubits by the collective atomic states

$$\begin{aligned} |0\rangle &= \otimes_{i=1}^N |g\rangle_i, \\ |1\rangle &= \left(1/\sqrt{N}\right) \sum_{i=1}^N |g_1 \dots f_i \dots g_N\rangle. \end{aligned} \quad (1)$$

The single qubit rotation in our scheme is implemented by a sequence of three laser pulses [27] as shown in Fig. 1(b): (i) The flip operation by a  $2\pi$  pulse, i.e.,  $[\int d\tau \Omega_f(\tau)/2 = \pi]$ , results in  $|f\rangle \rightarrow |r\rangle$ ; (ii) A coherent evolution between  $|r\rangle$  and  $|g\rangle$  by a  $2\phi$  pulse  $[\int d\tau \Omega_r(\tau)/2 = \phi]$ ; (iii) Another flip operation by a  $2\pi$  pulse results in  $|r\rangle \rightarrow |f\rangle$ . In the step (ii), the Rydberg blockade guarantees only a single excitation in the atomic ensemble.

If  $\phi = \pi$  or  $\pi/2$ , the single qubit rotation corresponds to the Pauli X or Hadamard gate. Moreover, the Rydberg states should be excited in a Doppler-free fashion, which can be accomplished using two counter-propagating laser waves. As the logical qubits can be rotated rapidly [18] and measured with high efficiency by

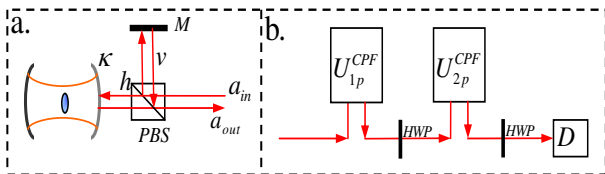


FIG. 2: (Color online) (a) Schematic setup for the basic building blocks. The single-photon pulse is injected into the cavity after passing through a PBS. The optical paths from the PBS to the cavity and to the mirror  $M$  are assumed to be equal, then the  $h$  polarization component reflected from the cavity can be superposed coherently with the  $v$  polarized component reflected via the mirror. (b) The CPF gate between two qubits. The box  $D$  includes a PBS and two single-photon detectors for the output.

resonance fluorescence detection [28], our scheme would be useful for one-way quantum computation [43], as discussed later.

### B. CPF gating between a single-photon pulse and the atomic ensemble

Combined with the Rydberg blockade, our basic building block for QIP works based on the cavity input-output process. As shown in Fig. 2(a), the atomic ensemble is trapped in a one-sided cavity. The atomic transition between  $|f\rangle$  and  $|e\rangle$  is coupled resonantly to the cavity mode  $a_h$  and also resonantly driven by the  $h$  polarization component of the input single-photon pulse. In the rotating frame with respect to the cavity frequency, the interaction of the atoms with the cavity mode is described by the Hamiltonian,

$$H = \sum_{i=1}^N (g_i a \sigma_+^i + g_i^* a^\dagger \sigma_-^i), \quad (2)$$

where  $\sigma_+^i = |e\rangle\langle f|$ ,  $\sigma_-^i = |f\rangle\langle e|$ ,  $g_i$  is the coupling rate between the  $i$ th atom and the cavity mode. For simplicity of treatment, we may assume  $g_i = g$  from now on. By adiabatically eliminating the cavity mode [39, 44], the cavity output  $a_h^{out}(t)$  corresponds to

$$a_h^{out}(t) = \frac{i\Delta - \kappa/2}{i\Delta + \kappa/2} a_h^{in}(t) \quad (3)$$

where  $\kappa$  is the cavity decay rate,  $\Delta$  is the detuning between the input photon and the dressed cavity mode, and  $a_h^{in}(t)$  is the one dimensional input field operator satisfying  $[a_h^{in}(t), a_h^{in\dagger}(t')] = \delta(t - t')$ . If the atomic ensemble is initially in the state  $|0\rangle$ , the Hamiltonian  $H$  does not work and thereby  $\Delta = 0$ . So we have

$$a_h^{out}(t) = -a_h^{in}(t). \quad (4)$$

In contrast, if the atomic ensemble is in the state  $|1\rangle$  and the input field senses the dressed cavity modes  $\Delta = \pm g$

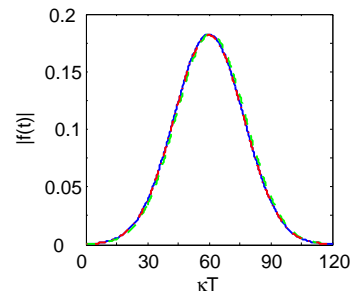


FIG. 3: (Color online) Pulse shape for the input pulse (solid line) and the output pulse of the single photon with the atomic ensemble qubit in the state  $|0\rangle$  (dashed line) and  $|1\rangle$  (dash-dotted line). The input pulse shape is assumed to be Gaussian with  $f_{in}(t) \propto \exp[-(t-T/2)^2/(T/5)^2]$ , where  $T/5$  is the pulse width. As they are nearly identical and nearly completely overlapping, the pulses are hard to be distinguished in the plot.

[39], in the case that  $g \gg \kappa$ , we get  $a_h^{out}(t) = a_h^{in}(t)$ . As a result, the output of the photon means an implementation of the CPF gate  $U_{ap}^{CPF} = e^{i\pi|0h\rangle\langle 0h|}$  between the single-photon and the atomic ensemble.

The same gating operation could also be achieved in weak coupling regime or in a bad cavity if we could set the values of the parameters appropriately. We will discuss this point later.

### C. The gate performance

In what follows, to quantitatively characterize the CPF gating, we will perform a numerical simulation by the method specified in [39] using the realistic parameters  $(g_0, \kappa, \gamma_s)/2\pi = (34, 4.1, 2.6)$  MHz [45]. Assuming the initial state of the total system to be  $|\Psi_{in}\rangle = \sum_i c_{ip} |i\rangle_a |p\rangle_i$  with  $i \in \{0, 1\}$  and  $p \in \{h, v\}$ ,  $\sum_i |c_{ip}|^2 = 1$ , where  $|p\rangle_i = \int dt f_{in}(t) a_p^{in\dagger} |vac\rangle$  is the input photon state with  $f_{in}(t)$  the input Gaussian pulse, we have the state of the output pulse to be  $|p'\rangle_i = \int dt f_{out}^{ip}(t) a_p^{out\dagger} |vac\rangle$  with  $f_{out}^{ip}(t)$  the output pulse shape. Normally, from the above model, we can directly obtain the result  $f_{out}^{0h}(t) = -f_{in}(t)$  and  $f_{out}^{ip}(t) = f_{in}(t)$  ( $ip \in \{0v, 1v, 1h\}$ ). Our simulation shown in Fig. 3 demonstrates that the output pulse shapes  $|f_{out}^{0h}(t)|$  and  $|f_{out}^{1h}(t)|$  overlap very well with the input pulse shape  $f_{in}(t)$ . Consequently, the fidelity  $F$  of the CPF gate is determined by the shape matching degree, as plotted in Fig. 4(a) where the gating is nearly with the fidelity up to 99.7% in the case that the pulse duration  $T$  is much larger than  $1/\kappa$ .

Furthermore, the gating fidelity is insensitive to the variation of the coupling rate. Although  $g$  varies by a factor of 2 due to the residual atomic motion in current experiments [45], the change of the fidelity in our calculation is only about  $10^{-3}$ . As a result, the atoms is not necessarily to be strictly localized within the Lamb-Dicke

regime. In our numerical simulation, an imaginary part  $-i\frac{\gamma_s}{2}\sum_{i=1}^N|e\rangle_i\langle e|$  is introduced to describe the atomic spontaneous emission rate  $\gamma_s$  in the Hamiltonian  $H$  in Eq. (2). With the typical choice  $g = 3\kappa$ , the leakage rate for a CPF gating is  $P_e = P_s/4 = 1.7\%$  (see Fig. 4(b)), which implies a high success probability of the gating.

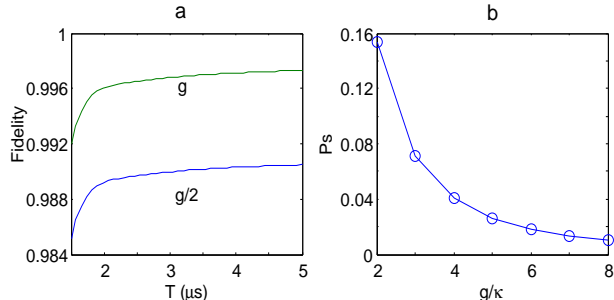


FIG. 4: (Color online) (a) The gating fidelity versus the pulse duration  $T$ . (b) The photon loss probability  $P_s$  due to the atomic spontaneous emission with respect to the coupling rate  $g$  in units of  $\kappa$ , where  $T = 120/\kappa$  is used and  $(g_0, \kappa, \gamma_s)/2\pi = (34, 4.1, 2.6)$  MHz.

### III. APPLICATION

#### A. Conditional gates between atomic ensembles

The above CPF gating between the atomic ensemble and the single-photon can be extended to nontrivial two-qubit gating between atomic ensembles as illustrated in Fig. 2(b), where  $U_{ap}^{CPF}$  ( $a = 1, 2$ ) box corresponding to the setup in Fig. 2(a) functions as the CPF gate between the atomic ensemble  $a$  and the single-photon. The single-photon pulse injected into the box is initially prepared in the state  $(|h\rangle + |v\rangle)/\sqrt{2}$  with  $|h\rangle$  and  $|v\rangle$  the photonic state with polarizations  $h$  and  $v$ , respectively. The pulse is reflected successively from the two boxes, with a half-wave plate (HWP) inserted into the optical path between the two boxes which performs the rotation  $|h\rangle \rightarrow (|h\rangle + |v\rangle)/\sqrt{2}$  and  $|v\rangle \rightarrow (|h\rangle - |v\rangle)/\sqrt{2}$ . The final output single-photon pulse after passing through a HWP is detected by its polarization corresponding to the measurement of the polarization in the basis  $\{|h\rangle \pm |v\rangle\}/\sqrt{2}$ .

By a straightforward algebra, one can easily find that, if the photon is detected in the state  $|h\rangle$ , the CPF gating  $U_{12}^{CPF} = e^{i\pi}|11\rangle_{12}\langle 11|$  succeeds. If the detection is made on the state  $|v\rangle$ , the CPF gating could also succeed after an additional single-qubit operation  $\sigma_x$  on the atomic ensemble 2. As a result, a CNOT gate, with the CPF gate sandwiched by two Hadamard gates, is available.

#### B. Cluster state preparation

Assume the atomic ensembles 1 and 2 to be initially prepared in the state  $|0\rangle_1|0\rangle_2$ , and then in the state  $|\varphi_0\rangle = |+\rangle_1|+\rangle_2$  by Hadamard gates with  $|+\rangle = (|0\rangle + |1\rangle)/\sqrt{2}$ . A CPF gating between the two atomic ensembles, as demonstrated in Fig. 2(b), yields a cluster state like,

$$|\varphi\rangle_{12} = \frac{1}{2}[(|0\rangle_1 + |1\rangle_1\sigma_z^2)(|0\rangle_2 + |1\rangle_2)] \quad (5)$$

with  $\sigma_z^i = |0\rangle_i\langle 0| - |1\rangle_i\langle 1|$ . This is to say, if the output photon is detected as described in above subsection, we obtain successfully the state in Eq. (5). The idea could be directly extended to many-qubit case. For instance, two pairs of atomic ensembles 1, 2 and 3, 4 have been prepared independently in the state  $|\varphi\rangle_{12} \otimes |\varphi\rangle_{34}$ . The two pairs of atomic ensembles could be connected by a CPF gate between the qubits 2 and 3, which yields a four-partite atomic cluster state,

$$|\varphi\rangle_{1-4} = \frac{1}{4} \otimes_{i=1}^4 (|0\rangle_i + |1\rangle_i \sigma_z^{i+1}), \quad (6)$$

where  $\sigma_z^5 \equiv 1$ . With the similar idea to above operations, we can efficiently generate an  $n$ -party atomic ensemble cluster state

$$|\varphi\rangle_{1-n} = \frac{1}{\sqrt{2^n}} \otimes_{i=1}^n (|0\rangle_i + |1\rangle_i \sigma_z^{i+1}), \quad (7)$$

with the convention  $\sigma_z^{n+1} \equiv 1$ . If the success probability of the CPF gate is  $p$  and the time for each attempt of the CPF gate is  $t_0$ , the total preparation time for an  $n$ -qubit cluster state is  $T_n \simeq t_0(1/p)^{\log_2 n}$ , a polynomial function of  $n$ , growing much more slowly than the exponential scaling in [31]. In realistic implementation, the interface between atomic ensembles and photons with high success probability favors a high efficiency of cluster state generation.

In fact, the one-dimensional (1D) cluster states are not sufficient for a universal quantum computation. Recent studies [46, 47] have shown a highly efficient generation of cluster states with any complex 2D lattice geometry even in the case of low success probability of the CPF gating. Following the ideas in [46, 47], if we have two sufficiently long cluster chains which can be done *off-line*, the state in  $+$ -shape [46] or in star shape [47] with identical legs could be generated as the building block of the 2D geometry by the shrinking and removing techniques on the cluster states. Taking the  $+$ -shape as an example, via a CPF gate operation, we may fuse the end qubits of one of the legs of the two  $+$ -shape cluster states. If it works, and there are still redundant leg qubits between the two center qubits in the shapes, we can remove the qubits by applying simple  $X$  measurements on the qubits (i.e., the removing technique). Simply repeating the procedure, an arbitrary 2D lattice geometry can be easily constructed. Due to the high success probability of the CPF gating in our scheme, we can achieve a much more efficient scaling than in previous schemes [46, 47].

### C. Quantum repeater and remotely controlled operation

Quantum communication over long-distance remains challenging due to exponential attenuation of the transmitted signals. Fortunately, quantum repeater could resolve the fiber attenuation problem, reducing the exponential scaling to polynomial scaling [1, 2, 3]. Following the Duan-Lukin-Cirac-Zoller model [2], the quantum repeater can also be realized in the present system with pairs of atomic ensembles trapped in separate cavities. By adiabatically changing the Rabi frequencies of the pumping and repumping pulses with a large detuning [2, 48], we can store and retrieve the information at will. Note that the scattered photon will go to some other optical modes other than the signal mode. However, when the atomic number  $N$  is large, the independent spontaneous emissions distribute over all the atomic modes, whereas the contribution to the signal light mode would be small, leading to a high signal-to-noise ratio  $R \sim 4Ng^2/\kappa\gamma_s$  [2]. As a result, the use of atomic ensembles as a quantum node could result in collective enhancement. Moreover, with the high-fidelity entanglement generated by the quantum repeater, the high-fidelity controlled operation can be realized between two remote quantum nodes, as shown in Fig. 5.

Besides quantum communication [2], we show below that the entanglement between two remote atomic ensembles  $E_1$  and  $E_2$  is useful for quantum gating between two remote atomic ensembles or between two atoms. This helps for distributed QIP. As an example, we show how to achieve a CNOT gate between two remote single atoms  $S_1$  and  $S_2$  (see Fig. 5). This can be understood by following identity

$$\begin{aligned}
& C_{S_1 E_1} C_{E_2 S_2} (|\psi\rangle_{S_1 S_2} |\varphi\rangle_{E_1 E_2}) \\
&= \sigma_x^{S_2} C_{S_1 S_2} |\psi\rangle_{S_1 S_2} \otimes |0\rangle_{E_1} |+\rangle_{E_2} \\
&\quad + (-\sigma_z^{S_1} \sigma_x^{S_2}) C_{S_1 S_2} |\psi\rangle_{S_1 S_2} \otimes |0\rangle_{E_1} |-\rangle_{E_2} \\
&\quad + C_{S_1 S_2} |\psi\rangle_{S_1 S_2} \otimes |1\rangle_{E_1} |+\rangle_{E_2} \\
&\quad + \sigma_z^{S_1} C_{S_1 S_2} |\psi\rangle_{S_1 S_2} \otimes |1\rangle_{E_1} |-\rangle_{E_2}, \quad (8)
\end{aligned}$$

where  $C_{AB}$  means a CNOT gate on qubit  $B$  conditional on  $A$ ,  $|\varphi\rangle_{E_1 E_2} = (|01\rangle_{E_1 E_2} + |10\rangle_{E_1 E_2})/\sqrt{2}$ ,  $|\pm\rangle = (|0\rangle \pm |1\rangle)/\sqrt{2}$ ,  $\sigma_z^i$  and  $\sigma_x^j$  denotes the single qubit Pauli operators acting on the corresponding qubits  $i$  and  $j$ . It can be easily seen that, the key step for the nonlocal CNOT gate is the local CNOT gate between atomic ensemble and single atom qubits, which could be accomplished by the similar steps in Section III(A). After implementing the local CNOT gate, we should measure the ensemble qubit  $E_1$  in the basis  $\{|0\rangle_{E_1}, |1\rangle_{E_1}\}$  and  $E_2$  in the basis  $\{|+\rangle_{E_2}, |-\rangle_{E_2}\}$ . The measurement results  $\{|0\rangle_{E_1} |+\rangle_{E_2}, |0\rangle_{E_1} |-\rangle_{E_2}, |1\rangle_{E_1} |+\rangle_{E_2}, |1\rangle_{E_1} |-\rangle_{E_2}\}$  corresponds to a single qubit operation  $\{\sigma_x^{S_2}, I, \sigma_z^{S_1} \sigma_x^{S_2}, \sigma_z^{S_1}\}$  on the single atom qubits. Making use of the atomic ensemble qubits and the photon-mediated interaction, we could achieve the

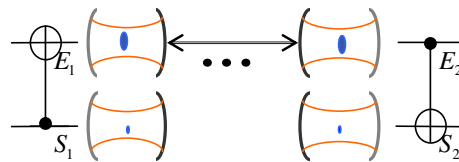


FIG. 5: (Color online) Schematic setup for CNOT gating between two remotely located single-atoms.

high-fidelity remote quantum CNOT gate between two single atoms. As a result, a high-fidelity long-distance entanglement is mapped to two single atoms, which can be used for faithful quantum state transfer over long distance [49]. This nonlocal gating also provides a basic tool for distributed quantum computation [50].

## IV. DISCUSSION

Whether the Rydberg blockade works well or not depends critically on the weakest interaction between the most apart atoms in the ensemble. As a result, it is important to choose appropriately the Rydberg state for carrying out our scheme. At a characteristic length scale of  $R_c$ , the usual van der Waals interaction could be treated as the Förster interaction. Then the Rydberg-Rydberg potential energy can be written as  $V_{\pm}(R) = \frac{\delta}{2} \pm \sqrt{\frac{\delta^2}{4} \pm D_{\varphi} \frac{C_3^2}{R^6}}$ , corresponding to the Förster resonant case  $ns_{1/2} + ns_{1/2} \rightarrow np_{3/2} + (n-1)p_{2/3}$ , the Förster defect  $\delta = E(np) + E((n-1)p) - 2E(ns)$ , the eigenvalue of the Schrödinger equation for the van der Waals interaction with fine structure  $D_{\varphi} = 1.333$ ,  $C_3 = \frac{e^2}{4\pi\epsilon_0} \langle np || r || ns \rangle \langle (n-1)p || r || ns \rangle$ ,  $R_c = (2C_3/\delta)^{1/3}$  [42]. As shown in Fig. 6(a), the 75s Rydberg levels gives  $V > 100$  MHz of blockade shift at a separation as large as  $5 \mu m$ . Considering the experimental condition  $\Omega_r/2\pi = 1$  MHz and  $V \gg \Omega_r$ , we may safely neglect the triply and higher excited states [51]. For several thousand atoms in the atomic ensemble, the probabilities of the zero and double excitation are about  $10^{-3} \sim 10^{-4}$  [51]. We have also calculated the fidelity of the CPF gate  $U_{ap}^{CPF}$  in Fig. 6(b) under the influence of double excitation. We found the fidelity still remaining as high as 99.2% in the case that the double excitation probability approaches  $P_2 = 0.01$ . In contrast, if  $P_2$  only varies from 0 to 0.01, the fidelity is insensitive to the double excitation probability.

In Section II, we have simply assumed the atoms to be collectively coupled to the cavity mode with a constant coupling rate  $g$ . However, the actual atom-cavity coupling depends on the atom's position  $\mathbf{r}$  through  $g(\mathbf{r}) = g_0 \cos(k_c z) \exp[-r_{\perp}^2/w_c^2]$ , where  $g_0$  is the peak coupling rate,  $r_{\perp}$  is the radial distance of the atoms with respect to the cavity axis,  $w_c$  and  $k_c$  are the width and the wave vector of the Gaussian cavity mode. With current experimental capabilities, the atoms can be confined inside a

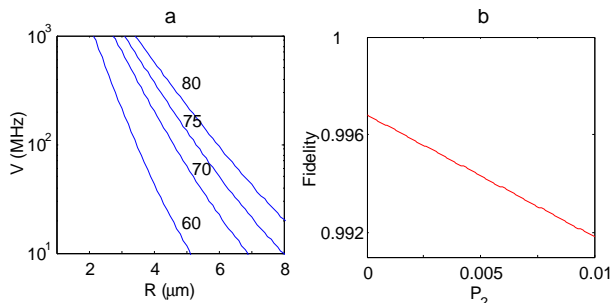


FIG. 6: (Color online) (a) The dipole-dipole interaction strength  $V$  with respect to atomic separation  $R$  for different Rydberg states. (b) The fidelity of the basic model shown as a function of the double excitation probability  $P_2$ . The parameters here are employed with the same values as in Fig. 4.

potential well along the cavity axis with a nearly fixed value of  $g(\mathbf{r})$ . But the intracavity fields of the FORT beam form many potential wells inside the cavity with different coupling rates in different potential wells. To implement our scheme to the best, we have to know precisely in which well the atoms are trapped [52].

Recent experimental advance [35] have achieved many atoms in a cavity with each atom identically and strongly coupled to the cavity. Based on the fiber-cavity and the atom-chip technologies, a BEC or cold cloud of  $^{87}\text{Rb}$  atoms in the  $5S_{1/2} |F=2, m_F=2\rangle$  ground state can be prepared and positioned deterministically within the cavity, and localized entirely within a single antinode of the tight optical lattice [35]. For a certain lattice site, a well-defined and maximal atom-field coupling could be achieved. If following the definition in [35] where  $\bar{g}^2 = \int d\mathbf{r} \rho(\mathbf{r}) |g(\mathbf{r})|^2 / N$ , with  $g(\mathbf{r})$  the position-dependent single-atom coupling strength, and  $\rho(\mathbf{r})$  the atomic density distribution, we could calculate the average value of the single-atom coupling rate  $\bar{g}$ . For a Gaussian cloud centered on a single lattice site with  $N < 1000$  and  $\bar{g}/2\pi = 200$  MHz, the fidelity of our CPF gate  $U_{ap}^{CPF}$  can approach 99.6%. In fact, the combined trap is of the flat disk shape [45, 53], in which the axial trapping frequency ( $\nu_z$ ) is much larger than the radial trapping frequency ( $\nu_{r\perp}$ ). By changing the power of the standing-wave field, we may have  $k_c \delta z \ll 1$ ,  $\delta r_\perp \ll w_c$ , then we have negligible variation of the coupling, i.e.,  $\delta g/g_0 \ll 1$ . To keep our qubits made of BEC, however, the axial trapping frequency of the lattice should be smaller than  $\nu_z = 20$  kHz [35].

We have noticed a recent experiment demonstrating the strong coupling of a  $^{87}\text{Rb}$  BEC to a ultrahigh-finesse optical cavity mode [36], in which the atoms in the  $^{87}\text{Rb}$  BEC occupy a single mode of the matter-wave field and couple identically to the light field. Inspired by another experimental advance with the Rydberg excitation of a  $^{87}\text{Rb}$  BEC [26], a  $^{87}\text{Rb}$  BEC may be employed to encode a qubit with the help of Rydberg blockade. Using the experimental values  $(g, k, \gamma_s)/2\pi = (10.6, 1.3, 3.0)$  MHz

[36], we have numerically obtained the fidelity up to 96% in Fig. 4(a) with our theoretical model. Due to the strong coherence of the BEC, our study gives rise to fascinating route with the BEC as the qubits for QIP in the future.

Suppression of the decoherence regarding the collective excitation is an important issue. In the case that the atom-atom distance is larger than the reduced optical wavelength of the cavity field [17], i.e.  $d = \sqrt{\pi(\delta r_\perp)^2/N} > \lambda/2\pi$ , the collective dephasing rate in our case is equal to in the single-particle case. Besides, to avoid the direct interaction between the atoms being in the ground state, the atom-atom distance should be larger than the radius of the atom in the ground state, i.e.,  $r_g \sim n_g^2 a_0$  with  $n_g$  the quantum number of the ground state and  $a_0$  the Bohr radius. For  $n_g = 5$ ,  $\delta r_\perp \sim 5 \mu\text{m}$ , and  $N \sim 10^3$ , we have  $\lambda d \sim 1/\pi$  and  $d/r_g \sim 210$ , implying a valid single-particle approximation. So previous methods for reducing decoherence in single-atom systems could probably be used in our case, and the key point for suppressing dephasing is resorted to a highly stable external magnetic field. In addition, errors due to the atom-number fluctuations can be ignored if  $\delta N (\sim 10) \ll N$ .

## V. EXTENSION TO THE WEAK COUPLING AND BAD CAVITY REGIME

Although the atomic ensemble could in principle expedite the operations due to the enhanced coupling strength, we have to mention that the confined atomic ensemble interacting with the flying photon does not enjoy this advantage because the corresponding coupling occurs between  $|f\rangle$  and the auxiliary level  $|e\rangle$ . In this sense, the ensemble qubit interacting with the single flying photon works as the same as the single atom. As a result, we still need to work in the high-Q cavity with the strong coupling regime to accomplish our scheme (See Sec II(B)).

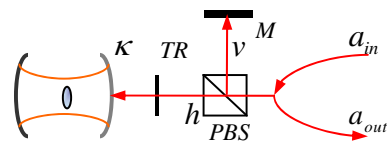


FIG. 7: (Color online) Schematic setup for implementation of the atom-photon CPF gate by twice reflections of the single-photon pulse in the weak coupling regime or in bad cavity. TR is the optical device exactly controllable for transmitting or reflecting a photon with very fast switch.

Based on a recent publication using Faraday rotation [54], however, we could extend our scheme to the cavity with low Q factor or with weak coupling. The key idea is the twice input and output of the flying single photon with respect to the cavity confining the atomic ensemble [55]. Since the Faraday rotation is produced

based on the state the atomic ensemble populating, we may achieve CPF gating under appropriate experimental parameters. For example, if the atomic ensemble is initially in the state  $|1\rangle$ , once a single-photon pulse is input, we may have the output single-photon pulse in the state  $e^{i\varphi}|h\rangle$  with  $\varphi$  the phase due to the Faraday rotation. In contrast, if the atomic ensemble is initially in the state  $|0\rangle$ , the single-photon pulse will sense a far-detuned cavity, yielding  $e^{i\varphi_0}|h\rangle$  with  $\varphi_0$  the Faraday rotating phase different from  $\varphi$  [54]. Supposing  $\omega_0 = \omega_c$ ,  $\omega_p = \omega_c - \kappa/2$ , with  $\omega_c$  and  $\omega_p$  the frequencies of the cavity and the single-photon, respectively,  $\omega_0$  the frequency difference between the levels  $|e\rangle$  and  $|f\rangle$  and  $\kappa$  the cavity decay rate, if in the weak coupling or the bad cavity case, i.e.  $g = \kappa/2$  and under the condition of the atoms staying forever in ground states (also corresponding to the negligible atomic decay rate [54]), we have the phase shift  $\varphi = \pi$  and  $\varphi_0 = \pi/2$  [54, 55]. With the single-photon pulse going in and out of the cavity twice, as shown in Fig. 7, we may have the atom-photon CPF gate  $U_{ap}^{CPF} = e^{i\pi|0h\rangle\langle 0h|}$  [55].

The single photon going through different cavities would yield the CPF gate between different atomic ensemble qubits [55], similar to the strong coupling and weak cavity-decay case discussed in Sec II (B). Therefore, the QIP tasks carried out in good cavities with strong coupling could also be accomplished in bad cavities or in weak coupling regime. The enhanced interaction strength due to the large number of the atoms could improve the efficiency in accomplishing one-way quan-

tum computing, quantum repeater and quantum state transfer. More importantly, it makes available to achieve quantum computation and quantum communication with sophisticated cavity QED technology [56].

## VI. CONCLUSION

In conclusion, based on an efficient quantum interface mechanism, we have shown a scalable ensemble-based QIP scheme. By encoding the qubits in the atomic ensembles within the Rydberg blockade range, we could have universal quantum gates with high success probability and high fidelity. We have also shown that our scheme could work well in either good or bad cavity and in either strong or weak coupling regime, which much reduces the experimental requirement.

## ACKNOWLEDGEMENTS

The authors acknowledge the fruitful discussion with Ming-Sheng Zhan, Yun-Feng Xiao, Hui Yan, Peng Xu, and Xiao-Dong He. This work is supported by the National Natural Science Foundation of China under Grant. Nos. 10404007, 10774163 and 60578055, by the State Key Development Program for Basic Research of China (Grant No. 2007CB925204 and 2009CB929604), and by NUS Research Grant No. R-144-000-189-305.

- 
- [1] H.J. Briegel, W. Dür, J.I. Cirac, and P. Zoller, *Phys. Rev. Lett.* **81**, 5932 (1998).
  - [2] L.-M. Duan, M. D. Lukin, J. I. Cirac, and P. Zoller, *Nature (London)* **414**, 413 (2001).
  - [3] Z.-S. Yuan, Y. A. Chen, B. Zhao, S. Chen, J. Schmiedmayer, and J.-W. Pan, *Nature (London)* **454**, 1098 (2008).
  - [4] C.H. van derWal, M.D. Eisaman, A. André, R.L. Walsworth, D.F. Phillips, A.S. Zibrov, and M.D. Lukin, *Science* **301**, 196 (2003).
  - [5] T. Chanelière, D.N. Matsukevich, S.D. Jenkins, S.-Y. Lan, T.A.B. Kennedy and A. Kuzmich, *Nature (London)* **438**, 833 (2005).
  - [6] B. Zhao *et al.* *Nature Phys.* **5**, 95 (2009); R. Zhao *et al.* *Nature Phys.* **5**, 100 (2009);
  - [7] A. Kuzmich, W.P. Bowen, A.D. Boozer, A. Boca, C.W. Chou, L.-M. Duan, and H.J. Kimble, *Nature (London)* **423**, 731 (2003).
  - [8] C.W. Chou, S.V. Polyakov, A. Kuzmich, and H.J. Kimble, *Phys. Rev. Lett.* **92**, 213601 (2004).
  - [9] Z.-S. Yuan, Y.-A. Chen, S. Chen, B. Zhao, M. Koch, T. Strassel, Y. Zhao, G.-J. Zhu, J. Schmiedmayer, and J.-W. Pan, *Phys. Rev. Lett.* **98**, 180503 (2007).
  - [10] C.W. Chou, H. de Riedmatten, D. Felinto, S.V. Polyakov, S.J. van Enk, and H.J. Kimble, *Nature (London)* **438**, 828 (2005).
  - [11] D.N. Matsukevich, T. Chanelière, S.D. Jenkins, S.-Y. Lan, T.A.B. Kennedy, and A. Kuzmich, *Phys. Rev. Lett.* **96**, 030405 (2006).
  - [12] B. Zhao, Z.-B. Chen, Yu-Ao Chen, J. Schmiedmayer, and J.-W. Pan, *Phys. Rev. Lett.* **98**, 240502 (2007).
  - [13] D.N. Matsukevich, T. Chanelière, M. Bhattacharya, S.-Y. Lan, S.D. Jenkins, T.A.B. Kennedy, and A. Kuzmich, *Phys. Rev. Lett.* **95**, 040405 (2005).
  - [14] H. de Riedmatten, J. Laurat, C.W. Chou, E.W. Schomburg, D. Felinto, and H. J. Kimble, *Phys. Rev. Lett.* **97**, 113603 (2006).
  - [15] J. Simon, H. Tanji, J.K. Thompson, and V. Vuletić, *Phys. Rev. Lett.* **98**, 183601 (2007).
  - [16] S. Chen, Y.-A. Chen, B. Zhao, Z.-S. Yuan, J. Schmiedmayer, and J.-W. Pan, *Phys. Rev. Lett.* **99**, 180505 (2007).
  - [17] M.D. Lukin, M. Fleischhauer, R. Côté, L.-M. Duan, D. Jaksch, J.I. Cirac, and P. Zoller, *Phys. Rev. Lett.* **87**, 037901 (2001).
  - [18] D. Jaksch, J.I. Cirac, P. Zoller, S. L. Rolston, R. Côté, and M.D. Lukin, *Phys. Rev. Lett.* **85**, 2208 (2000).
  - [19] D. Tong, S.M. Farooqi, J. Stanojevic, S. Krishnan, Y.-P. Zhang, R. Côté, E.E. Eyler, and P.L. Gould, *Phys. Rev. Lett.* **93**, 063001 (2004).
  - [20] K. Singer, M. Reetz-Lamour, T. Amthor, L.G. Marcassa, and M. Weidemüller, *Phys. Rev. Lett.* **93**, 163001 (2004).

- [21] K. Afrousheh, P. Bohlouli-Zanjani, D. Vagale, A. Muford, M. Fedorov, and J.D.D. Martin, *Phys. Rev. Lett.* **93**, 233001 (2004).
- [22] T. Vogt, M. Viteau, J.-M. Zhao, A. Chotia, D. Comparat, and P. Pillet, *Phys. Rev. Lett.* **97**, 083003 (2006).
- [23] T. A. Johnson, E. Urban, T. Henage, L. Isenhower, D.D. Yavuz, T.G. Walker, and M. Saffman, *Phys. Rev. Lett.* **100**, 113003 (2008).
- [24] C. S. E. van Ditzhuijzen, A.F. Koenderink, J.V. Hernández, F. Robicheaux, L.D. Noordam, and H.B. vanLindenvandenHeuvel, *Phys. Rev. Lett.* **100**, 243201 (2008).
- [25] M. Reetz-Lamour, T. Amthor, J. Deiglmayr, and M. Weidemüller, *Phys. Rev. Lett.* **100**, 253001 (2008).
- [26] R. Heidemann, U. Raitzsch, V. Bendkowsky, B. Butscher, R. Löw, and T. Pfau, *Phys. Rev. Lett.* **100**, 033601 (2008).
- [27] E. Brion, K. Mølmer, and M. Saffman, *Phys. Rev. Lett.* **99**, 260501 (2007).
- [28] M. Saffman and T.G. Walker, *Phys. Rev. A* **72**, 042302 (2005); M. Saffman and K. Mølmer *ibid.* **78**, 012336 (2008).
- [29] E. Brion, L.H. Pedersen, M. Saffman, and K. Mølmer, *Phys. Rev. Lett.* **100**, 110506 (2008).
- [30] H. Yan, G.Q. Yang, T. Shi, J. Wang, and M.-S. Zhan, *Phys. Rev. A* **78**, 034304 (2008).
- [31] M. Zwiery and P. Kok, *Phys. Rev. A* **79**, 022304 (2009).
- [32] M. Müller, I. Lesanovsky, H. Weimer, H. P. Büchler, and P. Zoller, *Phys. Rev. Lett.* **102**, 170502 (2009).
- [33] M. Saffman and K. Mølmer, *Phys. Rev. Lett.* **102**, 240502 (2009).
- [34] K. M. Svore, B. M. Terhal, and D. P. DiVincenzo, *Phys. Rev. A* **72**, 022317 (2005).
- [35] Y. Colombe, T. Steinmetz, G. Dubois, F. Linke, D. Hunger, and J. Reichel, *Nature (London)* **450**, 272 (2007).
- [36] F. Brennecke, T. Donner, S. Ritter, T. Bourdel, M. Köhl, and T. Esslinger, *Nature (London)* **450**, 268 (2007).
- [37] E. Urban, T.A. Johnson, T. Henage, L. Isenhower, D.D. Yavuz, T.G. Walker, and M. Saffman, *Nature Phys.* **5**, 110 (2009).
- [38] A. Gaëtan, Y. Miroshnychenko, T. Wilk, A. Chotia, M. Viteau, D. Comparat, P. Pillet, A. Browaeys, and P. Grangier, *Nature Phys.* **5**, 115 (2009).
- [39] L.-M. Duan and H.J. Kimble, *Phys. Rev. Lett.* **92**, 127902 (2004); L.-M. Duan, A. Kuzmich, H.J. Kimble, *Phys. Rev. A* **67**, 032305 (2003); L.-M. Duan, B. Wang, and H.J. Kimble, *Phys. Rev. A* **72**, 032333 (2005); Y.-F. Xiao, X.-M. Lin, J. Gao, Y. Yang, Z.-F. Han, and G.-C. Guo, *Phys. Rev. A* **70**, 042314 (2004).
- [40] Z.-J. Deng, M. Feng, and K.-L. Gao, *Phys. Rev. A* **75**, 024302 (2007); H. Wei, Z.-J. Deng, X.-L. Zhang, and M. Feng, *Phys. Rev. A* **76**, 054304 (2007); H. Wei, W.-L. Yang, Z.-J. Deng, and M. Feng, *Phys. Rev. A* **78**, 014304 (2008).
- [41] T.G. Walker and M. Saffman, *J. Phys. B* **38**, S309 (2005).
- [42] T.G. Walker and M. Saffman, *Phys. Rev. A* **77**, 032723 (2008).
- [43] H.J. Briegel, D.E. Browne, W. Dür, R. Raussendorf, and M. Van den Nest, *Nature Phys.* **5**, 19 (2009).
- [44] D.F. Walls, and G.J. Milburn, *Quantum Optics* (Springer-Verlag, Berlin, 1994).
- [45] A. Boca, R. Miller, K.M. Birnbaum, A.D. Boozer, J. McKeever, and H.J. Kimble, *Phys. Rev. Lett.* **93**, 233603 (2004).
- [46] L.-M. Duan and R. Raussendorf, *Phys. Rev. Lett.* **95**, 080503 (2005).
- [47] Q. Chen, J.-H. Cheng, K.-L. Wang, and J.-F. Du, *Phys. Rev. A* **73**, 012303 (2006).
- [48] G.-W. Lin, X.-B. Zou, X.-M. Lin, and G.-C. Guo, *Phys. Rev. A* **79**, 042332 (2009).
- [49] C.H. Bennett, G. Brassard, C. Crépeau, R. Jozsa, A. Peres, and W.K. Wootters, *Phys. Rev. Lett.* **70**, 1895 (1993).
- [50] D. Gottesman and I.L. Chuang, *Nature (London)* **402**, 390 (1999).
- [51] M. Saffman and T.G. Walker, *Phys. Rev. A* **66**, 065403 (2002).
- [52] S.J. van Enk, J. McKeever, H.J. Kimble, and J. Ye, *Phys. Rev. A* **64**, 013407 (2001).
- [53] D.S. Petrov, M. Holzmann, and G.V. Shlyapnikov, *Phys. Rev. Lett.* **84**, 2551 (2000); A. Görlitz *et al. ibid.* **87**, 130402 (2001).
- [54] J.-H. An, M. Feng, and C.H. Oh, *Phys. Rev. A* **79**, 032303 (2009).
- [55] Q. Chen and M. Feng, *Phys. Rev. A* **79**, 064304 (2009).
- [56] B. Dayan, A. S. Parkins, T. Aoki, E.P. Ostby, K.I. Vahala, and H.J. Kimble, *Science* **319**, 1062 (2008).